Balancing postural control and motor inhibition during gait initiation

Lorenzo Fiori [1,2], Surabhi Ramawat [2,3] , Isabel Beatrice Marc [2,3], Valentina Giuffrida [2,3], Alberto Ranavolo [1],

*Francesco Draicchio [1] , Pierpaolo Pani[3], Stefano Ferraina[3], Emiliano Brunamonti [3]**

[1]Department of Occupational and Environmental Medicine, Epidemiology and Hygiene, INAIL, Rome, Italy
[2]Behavioral Neuroscience PhD Program, Sapienza University, Rome, Italy
[3]Department of Physiology and Pharmacology, Sapienza University, Rome, Italy

**Correspondence: emiliano.brunamonti@uniroma1.it*

Emiliano Brunamonti, PhD
Department of Physiology and Pharmacology
Sapienza University
P.le Aldo Moro 5, Rome
Phone: 06 4969 0389

Abstract

This study explores the link between cancelling a prepared gait initiation in response to sudden environmental changes and maintaining body stability. To address this, we developed a gait initiation version of the Stop Signal Task (SST), a widely used tool for evaluating motor inhibition during different forms of action control. To understand the relevance of postural control during gait initiation and suppression, we evaluated the underlying changes in anticipatory postural adjustments (APA). We report that specific trial-level variables, like the time to initiate or cancel stepping, interacted with biomechanical factors such as the center of mass displacement relative to the base of support, impacting performance. We identified a critical biomechanical threshold beyond which halting the movement became improbable. These findings underscore the tight connection between limb action control and overall body equilibrium, providing a framework within an established motor control paradigm. By incorporating biomechanical elements into this model, we demonstrate its efficacy for simulating complex real-life scenarios. This approach defines essential variables for studying neural correlations between action and postural control, guiding the development of tools for injury prevention and rehabilitation devices for individuals with movement and posture impairments, including those suffering of neurodegenerative disorders.

Keywords*: Gait initiation, Postural control, Motor inhibition, Stop Signal Task*

Introduction

A primary purpose of posture control is to preserve body stability during voluntary movements and environmental interactions (Bonnetblanc et al., 2004; Cordo and Nashner, 1982; Gallagher et al., 2021; Leonard et al., 2009; Massion, 1994). Gait, as full-body movement, has been described as a 'controlled falling' (Perry, 1992) and this is especially true during gait initiation when the motor system must cope with the challenge of safely translating the body from a stable stationary state to a new one (Day and Bancroft, 2018; Yiou et al., 2017). Before the first step, to ensure stability, the nervous system executes a set of anticipatory postural adjustments (APA) to avoid perturbations dangerous for stability.

This already taxing sequence can become even more challenging when abrupt demands emerge from the environment. For instance, when a pedestrian is moving after the green traffic light but a car speeds trough the crossway. In this situation, the APA anticipating the movement need to be interrupted and the motor system to deal with both cancelling the movement and activate a process that guarantee the maintenance of the body equilibrium (MacKinnon, 2018; Mille et al., 2012). Thus, preventing falls during gait initiation is a complex process involving APA and requiring the evaluation of environmental and proprioceptive stimuli (Lord and Fitzpatrick, 2001; Pijnappels et al., 2010; Rogers et al., 2001; Rebecca J. St George et al., 2007; Uemura et al., 2013). While this dynamic has been widely studied, how APA are adjusted if the initial step cancellation is required it is still unknown.

Here we approached this problem by implementing a gait version of the Stop Signal Task (SST) focusing on the initial phases of control. The SST is a widely used paradigm that has provided concrete quantifications of several parameters of motor inhibition (Hannah and Aron, 2021; Logan and Cowan, 1984). These measures have been of relevance for evaluating the behavioral and physiological correlates of action control of simple movements (Hannah and Aron, 2021; Schall et al., 2017; Verbruggen et al., 2019). In a typical SST experimental setup, participants are instructed to start a movement in response to a Go signal, and to refrain from the movement if a Stop signal is presented during the reaction time (Brunamonti et al., 2012; Hannah and Aron, 2021; Jana et al., 2020; Mirabella et al., 2011, 2006; Pani et al., 2022; Raud et al., 2022). By referring to a race model, where a go and a stop process run one against the other toward a finish line, the outcome

in trials requiring inhibition can be accounted as the process that crossed this line first (Logan and Cowan, 1984). In this context, stopping a planned movement is easiest in trials with longer Go reaction time when the Stop signal occurs sufficiently before the movement onset or the reaction time to the Stop signal is fast. Different combinations of these variables could define the outcome of movement inhibition, with corresponding failures and successes.

If this model defines a general framework of motor inhibition, here we expect to observe these variables to determine when APA will be completed or cancelled. The recent observation that the reaction time to a stop signal computed for a finger keypress correlates with suppression of a balance recovery step (Rydalch et al., 2019) point towards this direction, but direct evidence is needed.

We tested this hypothesis by successfully measuring, at the single trial level, APA responses to both Go and Stop signals presented during gait initiation and highlighted that all the derived variables align well with the established framework of the race model. It provides valid evidence that this framework of motor control could be extended to naturalistic movements, as recently proposed (Hannah and Aron, 2021).

The present findings hold significant applied value. For example, in the context of healthcare for vulnerable individuals, such as elderly or Parkinsonian patients, framing the observed gait initiation parameters within a theoretical context could aid in planning specific therapeutic interventions and monitoring their efficacy (Yitayeh and Teshome, 2016) .

Results

APA changes capture the key parameters of gait initiation and inhibition at the single trials level

We asked 12 subjects to stand in a comfortable position in front of a monitor where visual stimuli were presented (Figure 1A). In most of the trials (Go trials, 70%), subjects were instructed to start walking using the right leg soon after the presentation of a Go signal. We considered the first step initiated when the heel released the contact from the floor. In a subset of trials (Stop trials, 30%), a Stop signal was presented at variable intervals (stop signal delay; SSD) from the Go signal. Successful Stop trials (Stop Correct) were characterized as the trials in which the subjects did not interrupt the contact with the floor and cancelled the planned step, while trials in which the step movement was initiated, after the presentation of the Stop signal, were classified as Stop Error trials. A staircase procedure, monitoring the behavioral outcome for each SSD value proposed, was used to ensure each subject had approximately 50% successful Stop trials (see Material and Methods). We observed that in a subgroup of the Stop Error trials the foot position was rapidly restored after the initial heel release. We labelled these trials as Stop partial Error trials (see Material and Methods), as previously suggested in other contexts (de Jong et al., 1990; Jana et al., 2020; Raud et al., 2022) .

Before the heel lift, a sequential activation of APA elements was observed, first involving the center of pressure (COP) and then the center of mass (COM). Figure 1B-C illustrates the COP and COM trajectories and their reciprocal relationship in each of the different behavioral outcomes.

Figure 1B (left column) illustrates, in a three-dimensional space, the temporal evolution of the anteroposterior and mediolateral displacement of the COP and COM in an example trial of the different behavioral conditions, from a participant performing the task. In Go trials (top panels), consistent with existing literature on step initiation and completion, we first observed a lateral shift of the COP towards the side of the stepping foot (the right foot in this study). This was followed by a lateral shift towards the supporting foot, and subsequently, forward progression, initiating first heel and then whole foot lifting. The COM followed these COP adjustments by initially shifting laterally and then forward. The rightmost panels of Figure 1B illustrates the relationship between these variables projected onto a mediolateral-anteroposterior-

plane The bottom panels of Figure 1B demonstrate that the presentation of the Stop signal elicited a modification of the temporal evolution of COP and COM displacement, which varied across different outcomes of Stop trials. By monitoring the velocity variation of these biomechanical events (see Material and Methods and Supplementary figure 2), we captured the time at which the COP and COM responded to the Go signal for movement initiation, marking the corresponding APA reaction time across all trial types. Additionally, by examining the change in COM and COP velocity profiles, we estimated the time at which APA adjustments were rectified in response to the Stop Signal (Reaction time to the Stop Signal). These adjustments were further evaluated in function of extension of the Base of Support (BOS) at the time of the APA Reaction time to the Stop Signal in the different Stop trials. The different Stop trials illustrated in Figure 1B are characterized by different lengths of Reaction time to the Stop signal, appearing shorter in Stop Correct and Stop partial Error trials compared to Stop Error trials. These changes were accompanied by a lowering of the extension of BOS. In the latter, the Reaction time to the Stop signal obtained from the COP (blue squares) occurs in a time very close to the time of heel lift (black squares), while that obtained from the COM (blue circles) occurs even later, projecting the COM outside the edges of the BOS. Once obtained these estimates from each trial, we investigated whether their distributions could account for the outcomes. Figure 1C lower illustrates for a participant the distribution of both the APA reaction time across the different trials—Go, Stop Correct, Stop Partial Error, and Stop Error— and that of the Reaction time to the Stop signal obtained by both the COP and COM trajectories during Stop trials. The figure confirmed that the reaction to both the Go and Stop Signal was first detected by the adjustments of COP (green and blue squares) and then by those of COM (green and blue circles). The figure also illustrates that the relationship between the APA onset time obtained by either the COP or COM was comparable and evidenced longer in the Go and Stop Correct trials respect to Stop Error and partial Error trials (green circles and squares). Similar relationship in the Reaction time to the Stop signal was observed in COP and COM between the different types of Stop trials. For these trials we observed longer Reaction to the Stop signal in Stop Error trials than in the Stop Correct and partial Stop Error trials (blue circles and squares). Figure 1 D illustrates on a mediolateral-anteroposterior projection plane of the COP and COM across trials average trajectories of each participant in the different

trial types, which evidences a consistent pattern of displacement of the trajectories between the participants in the different types of trials.

To summarize, the different behaviors detected during the gait version of the SST were defined by a different COP trajectory that in turn was reflected in the time evolution of COM displacement. Accordingly, we observed that variations of the different patterns of trajectories that captured the reaction times to the Go and Stop signals at a single trial level occurred with different latencies in the different types of trials.

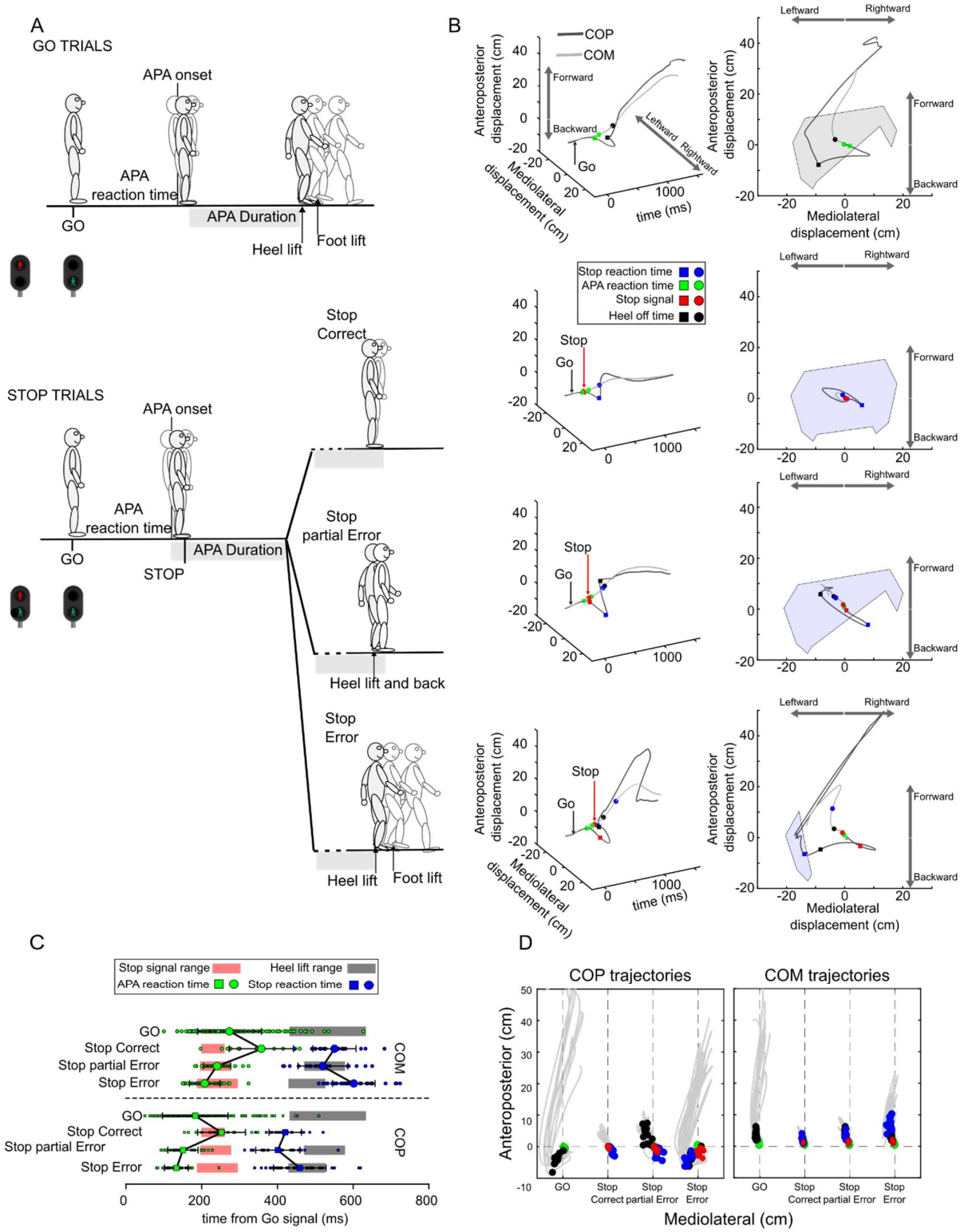

Figure 1 Illustration of the gait initiation stop signal task and trial by trial time evolution of COP and COM signals. A) A schematic of the behavioral outcome in the different task trials B) time course of the Mediolateral and Anteroposterior shifting of a single trial of the four possible outcomes in the task of a participant. Green squares and circles mark for each trial the time of APA onset obtained by the COP and COM respectively. In each stop trial, the time of Stop signal (red squares and arrows) and the corresponding reaction time (blue squares and circles) are indicated. The heel off time (dark square) in Go, Stop partial Error and Stop error trials are reported. Right panels also illustrate the extension of the BOS in Go trials at the time of heel lift (black area) and in Stop trials, at the time of the reaction rime to the Stop signal (light blue area). C) Displays the across trials distribution of the APA reaction time and the Reaction

time to the Stop signal for the representative participant in the different types of trials of a single participants. Average and s.e.m. of the different distribution is over-imposed to the distribution. Shaded grey areas mark the edges of the distribution of the heel lift time in Go, Stop partial Error and Error trials. Shaded pink areas marks the edge of distribution of the time of Stop signal onset in Stop trials. D) Illustration of the trajectory of COP and COM averaged across trials for the different behavioral outcomes in the 12 participants. The average of APA reaction time, time of Stop signal occurrence and Reaction time to Stop signal are projected on the 2D spatial displacement of the different trajectories.

Evaluation of the detected measures in the framework of the horse race model

The complex nature of a step initiation, involving a prolonged period of APA adjustments, offers a privileged window for observing motor variables supporting the framework of the Stop Signal paradigm developed through the study of ballistic or semi-ballistic movements (Atsma et al., 2018; Brunamonti et al., 2012; Brunamonti and Paré, 2023; Emeric et al., 2007; Mirabella et al., 2006; Paré and Hanes, 2003; Scangos and Stuphorn, 2010). In all these experimental contexts, a behavioral measure of the Reaction time to the Stop signal, commonly referred as Stop Signal Reaction Time (SSRT), is difficult to be obtained at a single trial level because inhibition refrains the overt movements. For the same reason, it is not possible to detect a reaction time to the Go signal in Stop Correct trials. Only recently, the trial-by-trial estimate of the SSRT in a few experimental studies has been obtained (Atsma et al., 2018; Goonetilleke et al., 2012; Jana et al., 2020; Jana and Murthy, 2018; Raud et al., 2022).

Here, we were able to measure these variables at the single-trial level by analyzing COP and COM trajectories (refer to Figure 1B and Material and Methods). We also tested whether these variables met the theoretical assumptions of the horse race model.

To this end, as a first step, we tested if our data satisfied the assumption of independence between the Go and Stop processes, hypothesized to run independently one from another after being triggered by a Go and a Stop signal, respectively (Logan and Cowan, 1984; Verbruggen et al., 2019). According to this model, the trials with the longer reaction times will be the ones that will be more likely inhibited by the occurrence of a stop signal (Logan and Cowan, 1984). Here we tested this assumption by comparing the COP and COM reaction time to the Go signal between Go and Stop trials.

Figure 2A shows that the longer APA (COP and COM, separately) reaction time to the Go signal were observed in the Stop Correct trials and Go trials, while the shorter reaction time was observed in both type of Stop Error trials. Moreover, the APA reaction times of the Stop partial Error trials were longer than those of Stop Error trials, a condition in line with the possibility to rectify a Stop trial initially started as Stop Error. This trend of the reaction times to the Go signal was similarly detected by considering either the time evolution

of the COP (Figure 2A: left panel) or the COM (Figure 2A: right panel). Within each set of measures, the differences between the Go reaction times were statistically significant. A one-way Anova revealed a significant difference between the distributions of the Go signal reaction time of COP ($F_{(1,3)}$= 127.40, p<0.001, η^2 = 0.98) and COM ($F_{(1,3)}$= 83.7, p< 0.001, η^2 = 0.97). Bonferroni post-hoc comparison detected for both COP and COM significant difference between each reaction time to the others (all p_s< 0.001).

A further variable accounting for the Stop trials outcome in this framework is the link between the increased duration of the Stop Signal Delay (SSD) and the lower probability of cancelling prepared movements. Figure 2B illustrates that the length of SSD of Stop Correct trials was significantly different between the different Stop trials (one-way Anova: $F_{(1,2)}$= 15.16, p< 0.001, η^2 = 0.88). Bonferroni post-hoc comparisons detected that Stop correct SSD were significantly shorter than Stop partial error and Stop error trials SSD (all p_s< 0.05). However, no significant difference was detected between SSDs of the Stop Error and Stop partial Error trials (p> 0.05).

Finally, we evaluated a further implication of the model that relates the SSRT to the outcome in Stop trials, a relationship that is rarely tested experimentally. In the context of the race model, the Reaction time to the Stop signal is expected to be longer in Stop Error trials than in Stop partial Error and Stop Correct trials. Considering the temporal resolution of our measures, here we were able to detect these variables in each different category of Stop trials (Figure 2 C and Table 1). A one-way Anova confirmed that the observed differences were statistically significant (COP: $F_{(1,2)}$= 124.08, p< 0.001, η^2 = 0.98; COM: $F_{(1,2)}$= 144.35; p< 0.001, η^2 = 0.99; all Bonferroni post-hoc comparisons: p_s< 0.05).

Table 1

	COP	COM
Stop Correct	167(25)	309(32)
Stop partial Error	154(22)	286(22)
Stop Error	223(18)	388(29)

Computed SSRT in COP and COM. Mean (SD).

To verify that our measure of the APA Reaction time to the Stop signal complied with the theoretical horse race model, we correlated this variable, averaged across trials, with the SSRT estimated based on the model's assumption and the related computational method (See Materials and Method). We observed a significant correlation between these two measures of inhibition (Figure 2C). For both COP and COM, we detected a significant correlation coefficient between the SSRT estimated by the race model's assumptions and the one obtained by the APA displacement in the Stop Correct, Stop partial Error and Stop Error trials.

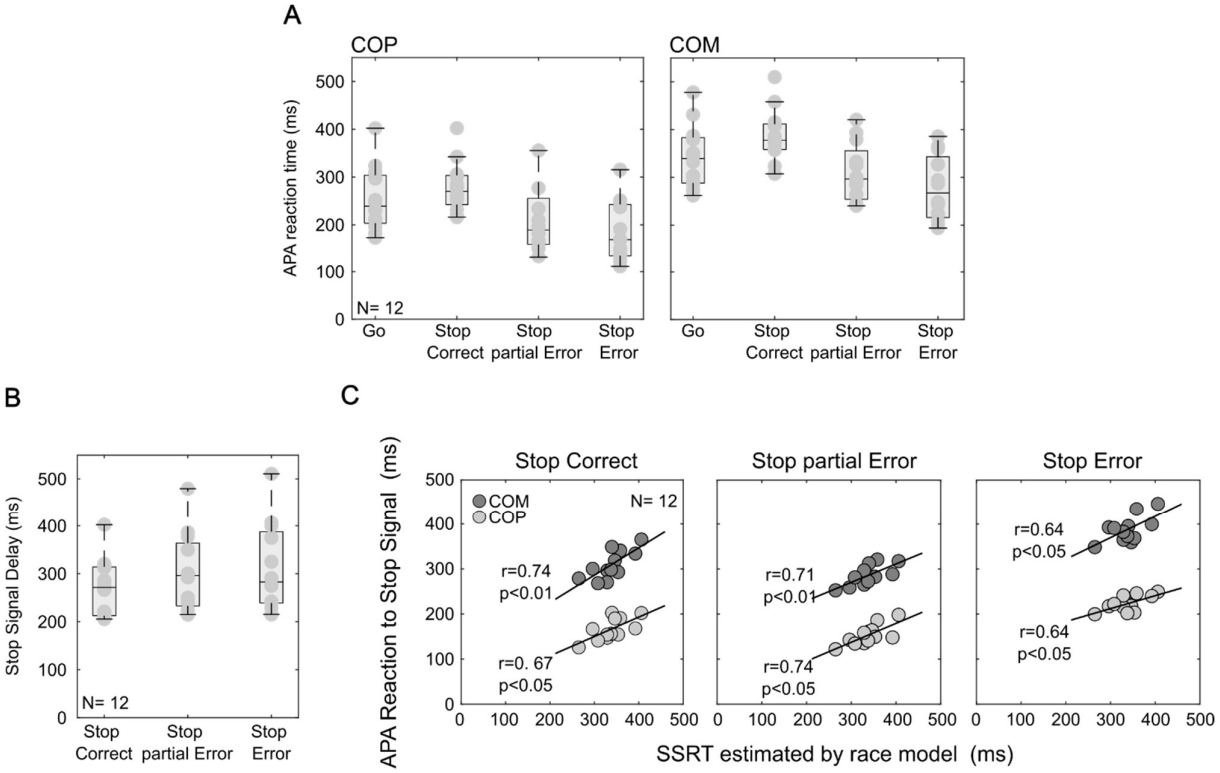

Figure 2

Stop signal task parameters estimated by the assumptions of the race model and the ones detected from the temporal evolution of the COP and COM. A. Boxplot comparing the APA reaction time to the Go signal between Go, Stop Correct, Stop partial error, and Stop error trials, detected in COP (left panel) and COM (right panel). B. Stop signal delay distribution in the different Stop trial categories for each of the different considered parameter C. Correlation analysis between SSRT estimated by the race model and the Reaction time to the Stop signal obtained by the kinetic ad kinematic signals.

Failure in canceling the step depends on the biomechanics of the body at the time of stop reaction

Our approach allowed us to detect, on the base of APA measures displacement, a Reaction time to the Stop signal, at single trial level, that significantly correlated with the behavioral estimate of the SSRT based on the race model assumptions as a reliable estimate of this parameter of inhibition. Since this reaction occurred in each of the different categories of Stop trials, here we asked when this ended up with a successful inhibition of the step initiation. To answer this question, we compared the area of the base of support (BOS; see Materials and Method) and the vertical projection of the COM on it (XCoM). Figure 3 shows that if at the time of the detected Reaction time to the Stop signal the XCoM fell within the area of BOS the step was successfully cancelled. This is the case of Stop Correct and Stop partial Error trials for which the inhibitory signal kept the body in the starting position (Figure 3 A-B). On the contrary, in Stop Error trials, the reduced area of BOS (Figure 3 A rightmost panel) did not allow the maintenance of the starting position. In these trials the loss of equilibrium was prevented by a forward step that increased the area of BOS (not shown). Across participants, we detected the antero-posterior and mediolateral displacement of COM (measured as Stability index; see Materials and Methods) in Stop Error trials was approximately 3 times, and significantly different, to that of Stop Correct and Stop partial Error trials (Figure 3 B).

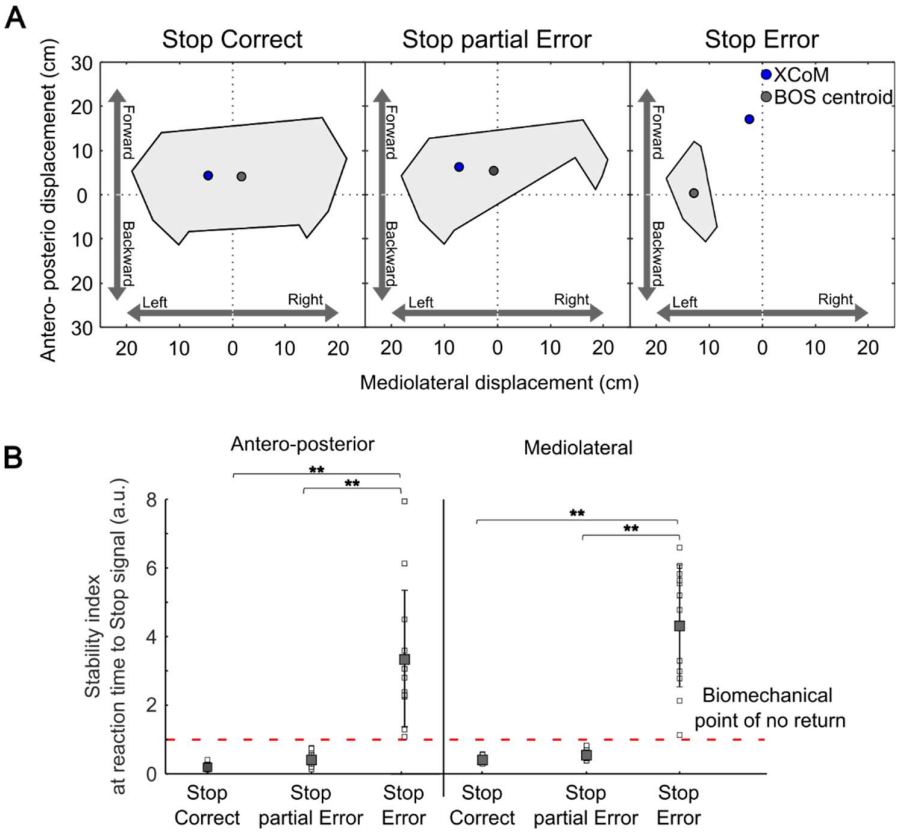

Figure 3

Relationship between the BOS and COM at the time of the reaction to the Stop signal. A. Antero-posterior and mediolateral displacement of COM at the time of stop reaction time. B. Stability index calculated at the Reaction time to Stop signal in the three different categories of Stop trials. One way Anovas (antero-posterior: $F(2)=29.0$, $p<0.001$; mediolateral: $F(2)=54.3$, $p<0.001$) and Bonferroni post-hoc comparisons ($ps< 0.05$) revealed a significant difference between the Stop error trials and both Stop correct and Stop partial error trials. Significant differences between the latest were not detected ($p>0.05$).

Discussion

In the present work, we implemented a gait initiation stop signal task to investigate how complex movement could be integrated in the framework of the stop signal paradigm. By extracting a set of variables from the monitoring of APA preceding the first step onset, we illustrate a scenario in which all detected variables—including the latency of APA reaction time to the Go and Stop signal, as well as the Stop Signal Delay duration—potentially influence step inhibition. Specifically, we observed that any combination of the detected variables that allows for the correction of APA while keeping the projection of the center of mass within the boundary of the base of support will result in successful step inhibition. We found that step inhibition depends on a point of no return determined by the biomechanical state of the body.

The great majority of studies on motor control have used experimental settings where relatively simple movements as key press or reaching to a peripheral target (Kalidindi and Crevecoeur, 2023) . Similar experimental settings have been employed for studying motor inhibition (Atsma et al., 2018; Brunamonti et al., 2012; Hannah and Aron, 2021; Mirabella et al., 2006). However, all ignored to evaluate the contribution of the postural adjustments often necessary. On the contrary, several of our daily actions (Bonnetblanc et al., 2004; Cordo and Nashner, 1982; Lowrey et al., 2017), require a simultaneous adjustment of the posture for allowing the proper completion of a movement. Recently APA have been described during reaching movements in crouched body posture (Gallagher et al., 2021). In the present study, we focused on step initiation, a complex behavior requiring a timely coordinated sequence of postural adjustments (Lepers and Breni�re, 1995; Yiou et al., 2017). While previous studies have addressed how the processing of external stimuli can affect the temporization of APA before starting a step (Lord and Fitzpatrick, 2001; Pijnappels et al., 2010; Rogers et al., 2001; R. J. St George et al., 2007; Uemura et al., 2013), our focus here is on how APA are modified when an external event leads to an efficient cancellation of the prepared gait initiation. By referring to the theoretical assumptions underlying the stop signal paradigm, here we outlined a framework that well embedded the possible behavioral outcomes occurring when the cancellation of a prepared step is required. Firstly, here we demonstrated that theoretical assumptions of the horse race model, developed from the study of simpler movements, well fitted such a complex motor behavior. Within this framework,

we found that trials with longer APA reaction times to the Go signal were more likely to be interrupted, particularly when a Stop signal was presented after a short SSD, and the APA Reaction time to the Stop signal was rapid. Crucially, we noticed that successful movement inhibition only occurred when these events aided in adjusting the movement until the COM did not cross a biomechanical threshold. Within this range of adjustment, all countermanding commands worked to maintain the body in a stable starting position. This was observed in Stop Correct and partial Error trials. In the former, the longer APA reaction time to the Go signal, as detected in the displacement of COP and CPM variations coupled with an earlier occurrence of the Stop signal at a shorter SSD, facilitated movement cancellation with minimal perturbation to body stability and kept the COM within the base of support boundaries. This correction was also aided by a short Reaction time to the Stop signal.

In Stop partial Errors, the COP and COM reacted earlier to the Go signal, and the Stop signal occurred at a longer SSD. However, the rapidity of the SSRT in these trials helped maintain the initial body position despite a perturbation that caused heel lift. As in previous trials, successful inhibition occurred because, at the time of the Reaction to the Stop signal, the COM's projection fell within the edges of the BOS. Finally, in Stop Error trials, the earlier COP reaction time to the Go signal and the occurrence of the Stop signal at a longer SSD were not counteracted by the SSRT duration. In fact, in these cases, the longer SSRT duration caused a deviation to the COP trajectory, which was reflected in the COM trajectory when it moved well outside the BOS boundaries. In this scenario, the only way to prevent falls was to complete the initiated step.

The present results fit previous findings, emphasizing a sequential progression of events leading up to the observable initiation of a movement, such as a key press. This progression starts with neuronal activity programming the movement and culminates in the engagement of muscular activity (de Jong et al., 1990; Jana et al., 2020; Raud et al., 2022). In Figure 4 we present a schematic that integrates our observation on APA with the theoretical background of the stop signal paradigm. This figure illustrates the dynamic interaction between the Go and Stop processes, which ultimately determine behavioral outcomes and contribute to estimating the Stop-Signal Reaction Time (SSRT) (as evidenced by the top reaction time distributions). Recent research (de Jong et al., 1990; Jana et al., 2020; Raud et al., 2022) has shown that

reaction times to both Go and Stop signals, based on movement onset, tend to overestimate the actual response to these signals, obscuring the temporal dynamics of the stop process and failing to provide insight into its completion time. Our results support the hypothesis that every Stop signal initiates the stop process, but its effectiveness in halting depends on the timing of its intervention and potential to rectifying the ongoing APA.

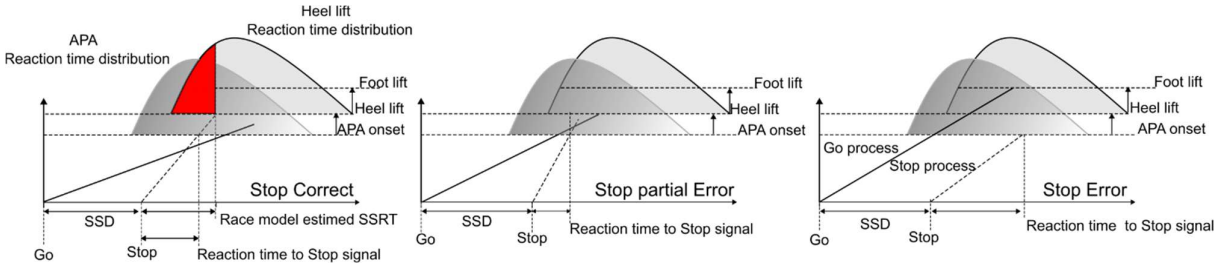

Figure 4

Biomechanical variables at play in step inhibition. Time evolution of the Go and Stop process in relation to the APA onset and Heel lift Reaction time distributions. In Stop correct trials (Left panel) the Stop process passes the threshold corresponding to the APA onset first. The APA reaction time to the Go signal could be still detected but there is no generation of movements. In Stop partial Error trials (Middle panel), the Go process is more rapid and, therefore, could pass both the APA and Hell thresholds. However, the Stop process is still sufficiently rapid to allow for a correction and the step is aborted. In the Stop Error trials (Right panel), the stop process is too slow and cannot compete with the Go process passing all the thresholds and generating the full step.

Implication for extending the stop signal paradigm to study complex movements and the underlying neural correlates

The present approach has yielded two significant achievements in the investigation of action inhibition using the Stop Signal Task. Firstly, we successfully detected important variables at the single-trial level, such as reaction time to the Go signal in Stop trials and the reaction time to the Stop signal in Stop Error trials. These variables were not previously identified in most studies even if their detection is crucial for evaluating the ongoing of movement's initiation and cancellation. Tentative SSRT detection at the single-trial level successfully estimated this variable in ballistic and semi-ballistic movements. This estimation was achieved by monitoring the activity of agonist or antagonist muscles involved in the task (Atsma et al., 2018; Jana et

al., 2020; Raud et al., 2022). In the case of finger movements, the SSRT measurement was obtained by identifying partial error trials. These trials represented a subset of Stop Correct trials where there was an initial increase in agonist muscle activity after the Go signal, as for starting a movement, followed by a decrease in activity to maintain the finger in the starting position as a response to the Stop signal. These findings indicated the existence of a point of no return, beyond which movement cancellation was unlikely, and provided an estimate of the SSRT based on the onset of muscle activity attenuation (Jana et al., 2020; Jankowska and Edgley, 1993; Raud et al., 2022).

Even in the present work we detected a subset of Stop partial Error trials that provided a reliable estimate of the SSRT. Here Stop partial Error trials were a proportion of Stop Error trials where the heel left the starting position, but the participant was still in the condition to refrain from movement generation. In addition, thanks to the monitoring of APA time evolution, here we were able to detect changes in velocity of the COP and COM trajectories that reliably estimated this variable also in Stop Correct and Stop Error trials. These measures, accounted for the hypothesis that only the attempts to cancel a programmed movement occurring before a point of no return can end up with a success. Importantly our results strengthen the hypothesis of a point of no return in movement control facing against the original hypothesis that correctly inhibited response in the SST were those corresponding to a partial preparation that never reached an overt manifestation even in absence of a stop signal (de Jong et al., 1990). This evidence strengthens the plausibility of the original formulation of the race model assuming the stop process to be triggered every time a stop signal is presented and challenges the hypothesis that stop failure is accounted by the occurrence of “trigger errors” (Bissett et al., 2021; Skippen et al., 2019). The present results reflect what recently observed in the dynamic of the neuronal activity in the Dorsal premotor cortex of monkey performing a reaching version of the SST. In that case, a movement was not initiated until the dynamics of the neuronal network was maintained within the boundary of a given configuration. Movements started only when the network crossed this boundary (Pani et al., 2022) . Here, we observed at a behavioral level that the relation between the body kinematics and the BOS marked a boundary between a control and a ballistic state for this behavior.

Accordingly, models of APA control hypothesized a role in of premotor areas in programming and rectifying these set of postural adjustments (see (Takakusaki, 2017, 2013) .

Our findings plausibly indicate that after having integrated biomechanical variables influencing the body stability in models of motor control it will be achieved a reliable understanding of environmental interaction in contexts closer to real life situations (Aron et al., 2014; Hannah and Aron, 2021). Understanding the roles of these variables in action inhibition is crucial for investigating the role played by each node of the neural circuits subtending action inhibition as the frontal cortex and premotor cortex (Aron et al., 2014; Mirabella et al., 2011; Scangos and Stuphorn, 2010) or the cerebellum (Brunamonti et al., 2014; Middleton, 2000; Olivito et al., 2017) . The importance of proprioceptive feedback influencing postural control (MacKinnon, 2018), as well as the managing of these afference by the spinal cord (Takakusaki, 2017, 2013) , subcortical nervous structure (Houk et al., 2007; Mori, 1987) or the somatosensory cortex (MacKinnon, 2018; Takakusaki, 2017, 2013) will enrich the understanding of the neural circuit managing complex behavioral adjustments.

To conclude, we obtained direct measurements of critical variables involved in postural adjustments during the initiation of steps that fit within a consolidated theoretical model of motor control. Considering the opportunity to monitor online variations of these variables, we draw the possibility of predicting the outcome of complex movements. These results provide a solid framework for designing and testing tools for accident prevention and the rehabilitation of neurological patients with posture control impairments, such as those suffering of Parkinson's disease (Yitayeh and Teshome, 2016).

Acknowledgments: *The authors are grateful to Dr. Isaac Kurtzer for valuable discussions.*

Author contributions: *L.F. collected and analyzed the data. L.F., S.R, I.B.M., V.R, F.D. and A.R. discussed the results and commented on the manuscript. E.B., P.P., S.F., F.D. and A.R. contributed to the study design. E.B., L.F., P.P., S.F. wrote the manuscript.*

Participants

Twelve healthy participants (4 women, 8 men) aged 33.3±7.1 years, with an average weight of 69.3 ±17.0 kg, and an average height of 169.7±8.2 cm, were recruited for the study. None had orthopedic or neurological issues or ongoing drug therapies. They provided informed consent. Participants completed a preliminary test using a revised Edinburgh Handedness Inventory (EHI) to determine preferred starting limb for walking (Oldfield, 1971). The study adhered to the Declaration of Helsinki and was approved by the local Ethics Committee (N. 0078009/2021). Data collection took place at the movement analysis laboratory, Department of Occupational and Environmental Medicine, Epidemiology and Hygiene, INAIL, research center in Monte Porzio Catone, Rome.

Gait initiation stop signal task

Each participant was initially positioned on two out of eight dynamometric platforms, with their feet parallel and bare, aligned with the movement analysis lab's x-axis following the International Society of Biomechanics' standard (Wu and Cavanagh, 1995). Subsequently, a contact sensor was inserted between the platform and the heel of the participant's preferred limb, while a computer monitor was positioned 2 meters away and 0.7 meters high for visual stimulus presentation. Participants received instructions to maintain focus on the stimulus monitor and initiate forward movement as quickly as possible. Before the experiment, participants underwent practice trials to familiarize themselves with the setup. Each gait initiation trial commenced when the participant's heel made contact with the sensor, triggering the stimulus system to display a traffic light signal on the monitor's center. This signal was then replaced, after a variable delay (randomly between 1 and 1.5 seconds), by a forward-facing arrow (595x822 pixels) acting as a Go signal.

In 70 % of trials required participants to initiate forward movement (Go trials). The initiation was determined by the release of sensor-heel contact, marking the participant's Heel lift time (RT). Go trials with an RT exceeding one second or occurring before the Go stimulus were considered ineligible.

In 30% of trials (Stop trials), the forward-facing arrow was replaced by a stop road sign (1024x1024 pixels), serving as a Stop signal. Upon presentation of the Stop signal, participants were instructed to halt their motor response and remain stationary. The Stop signal followed a variable delay from the Go signal (Stop Signal Delay; SSD), determined using a scaling algorithm based on participants' performance. The SSD, initially set at 50 ms, was adjusted automatically, increasing by 50 ms after each successfully cancelled Stop trial and decreasing by 50 ms following an uncanceled Stop trial, as per the algorithm. A trial was deemed a Stop Error trial if the participant lifted their heel from the contact sensor after the Stop signal; otherwise, it was a Stop Correct trial. Participants received auditory feedback on the correctness of their response. Each participant completed 10 blocks of 30 trials (300 trials in total), with SSD values maintained across consecutive blocks.

INSTRUMENTATION

In this experimental study, two systems were combined into one to capture both the behavioral and motor patterns linked to gait initiation. One system focused on movement analysis, collecting kinematics, dynamics, and muscle activity data, while the other managed behavioral aspects, handling visual and auditory stimuli and recording participant responses. These systems were synchronized to create an integrated and timed dataset. Only kinetic and kinematic data were analyzed in this study.

Behavior instrumentation

The SST paradigm was controlled by a PC running Windows XP, a monitor (18”), and a loudspeaker system. An algorithm implemented in the MATLAB computing environment managed the projection of visual stimuli on the screen and acoustic stimuli on the speakers, as well as the acquisition and transmission of information about both the emitted stimuli and the behavior of the participants via the sensor under the heel via a parallel port.

Gait Initiation recording instrumentation.

A stereo-photogrammetric motion analysis system with optoelectronic technology was used to collect the kinematics data (SMART-DX 6000 system: BTS, Italy, Milan). Eight infrared cameras with a sampling rate of 340 Hz were employed, as well as 33 reflective markers were placed above the anatomical reference points (Davis et al., 1991; Rab et al., 2002). In detail, the markers were placed above on the cutaneous projections of spinous processes of the seventh cervical vertebra, tenth dorsal vertebra, vertebra sacral, notch between clavicles and bilaterally on the frontal and parietal bones, inion, acromion, lateral humeral condyles, radial processes, ulnas styloid, third metacarpal, superior anterior iliac spine, and above the lower body bilaterally on the cutaneous projections of large trochanter, lateral femoral condyle, fibula head, lateral malleoli, head of the third metatarsus and heels (Supplementary figure 1 A).

This whole-body marker placement protocol, as well as the large number of markers used, were chosen to obtain a measurement of whole-body kinematics. This decision was made to be able to use the segmental

method to calculate the Center of Mass (COM; method explained later), which is evidently one of the most accurate methods for its estimation(Gutierrez-Farewik et al., 2006; Ranavolo et al., 2017) .

The kinetics data of the ground reaction forces (GRFs), with their center of pressure, were acquired using eight dynamometer platforms (Kistler 9286B; Kistler, Winterthur, Switzerland) at a sample rate of 680Hz (Supplementary figure 1 B). Each platform was made up of four load cells, with capacitive technology, each of which was placed in one of the platform's four corners. The peculiarity of these eight platforms was that they were virtually interconnected, so that the system could be considered as a single force platform during data extraction.

DATA ANALYSIS

3D reconstruction software (SMART Tracker and SMART Analyzer: BTS, Italy) and MATLAB (R2019b 9.7; MathWorks, USA) were used to process the kinematics and kinetics.

Classification of Stop partial Error and Error trials

During data collection, we found two types of Stop Error trials. In one, participants lifted both heel and toe, completing the movement. These were classified as Stop Error trials. In the other, only the heel was lifted without moving the limb forward. Similar to finger versions of the SST, these trials initially started as errors but corrected during the trial, akin to Stop partial Error trials (Jana et al., 2020; Raud et al., 2022) analyzed separately from regular Stop trials.

Operationally, we imposed a 5 cm threshold on the advancement of the malleolus marker to biomechanically characterize Stop partial Error:

$$\begin{cases} Partial\ Wrong & mall_x \leq 5\ cm \\ Wrong & mall_x > 5\ cm \end{cases}$$

Kinematic and kinetic pre-processing

To obtain an ordered and homogeneous collection of all Gait Initiation data, only a temporal window from 0.2 s before the Go signal until 1.6 s after it was studied. This time window ensures a thorough examination of APAs in all the studied participants' behavioral responses.

To keep only the signals of interest, all raw kinematics and kinematics data were first low-pass filtered with a zero-lag fifth-order Butterworth filter with a 10 Hz frequency of cut off.

Computation of the center of mass and the center of pressure

The pre-elaborated kinematics data were then used to evaluate the total body COM by combining them together with the subjects' anthropometric data and the estimate of body segment parameters(de Leva, 1996; Zatsiorsky and Aktov, 1990).

The computation was carried out by treating the COM as the centroid of a set of *n* body segments and computed as follows:

$$CoM(t) = \begin{cases} COM_x(t) = \dfrac{1}{m}\displaystyle\sum_{i=1}^{n} x_i(t) * m_i \\ COM_y(t) = \dfrac{1}{m}\displaystyle\sum_{i=1}^{n} y_i(t) * m_i \\ COM_z(t) = \dfrac{1}{m}\displaystyle\sum_{i=1}^{n} z_i(t) * m_i \end{cases}$$

Where, $COM_x(t)$, $COM_y(t)$ and $COM_z(t)$ are the instantaneous components of the $COM(t)$ position along the *x* (anteroposterior direction), *y* (mediolateral direction) and *z* (vertical direction) axes respectively; *m* is the mass of the system under consideration (weight of the subject), n is the total number of body segments under consideration (*n* = 12; head, trunk, 2 arms, 2 forearms, 2 hands, 2 legs, and 2 feet); while $x_i(t)$, $y_i(t)$ and $z_i(t)$ are the coordinate in the space of the *i-th* segment, and m_i is its mass.

The COP position was calculated from the distribution of the GRFs on the platforms as the point location of the ground reaction force vector and was directly released by motion analysis system, and computed as follows:

$$COP(t) = \begin{cases} COP_x(t) = \dfrac{M_y(t) + F_x(t) * d_z}{F_z} \\ COP_y(t) = \dfrac{M_x(t) - F_y(t) * d_z}{F_z(t)} \end{cases}$$

where $COP_x\ (t)$ and $COP_y\ (t)$ represent the instantaneous location of the $COP(t)$ on the force platform along the axes *x* (anteroposterior direction) and *y* (mediolateral direction), respectively; $M_x(t)$ and $M_y(t)$ are the moment of the force platform along *x*-axis and *y*-axis; $F_x\ (t)$, $F_y\ (t)$ and $F_z(t)$ represent the force in *x*-axis, *y*-axis, and *z*-axis, respectively, and d_z represents the height of the top of plate above measurement plane (*xy*).

Trial-by-trial detection of reaction time to the Go and Stop signal from the time evolution of COM and COP trajectories

A template-based algorithm was developed to automatically recognize the reaction times to Go and Stop stimuli from CoM and CoP trajectories. This technique is widely used in the literature to identify motor patterns in motion analysis signals (motion capture, inertial, surface electromyography, etc.)(Gan Huang et al., 2010; Muscillo et al., 2011; Oudre et al., 2018; Suzuki, 1995) .

Here, the template model was calculated and then applied to the velocity of the COM and COP. The velocity of COM and COP was calculated using finite difference derivatives and low-pass filtering of signals obtained with a zero-lag third-order Butterworth filter with a cut-off frequency of 5 Hz.

Template-based detection of reaction time to Go and Stop signal

To identify each participant's reaction to the Go signal, indicating the onset of APA, two templates were created, one for the COP and a second one for the COM trajectories (COM, COP), regardless of the type of trial. The templates were created by averaging five trials drawn at random from the Go trial dataset aligned to the Go signal. The velocity of the COM and COP trajectories was computed for each of the five trials were specifically after which the average signal was calculated and each one was appropriately trimmed based on the baseline variation at the start of the signal. The template built on the Go trials was used to capture the Reaction time to the Go signal for each Go and Stop trial.

For the stop trials, three templates were created for each signal (COM, COP) to identify the reaction time to the Stop signal: one for Stop Correct, a second for Stop partial Error, and a third for Stop error trials. Each template was generated by averaging three trials from each type of stop task behavior, randomly selected from the dataset and aligned to the time of stop presentation. Subsequently, the three signals were averaged and appropriately trimmed based on the signal.

Supplementary figure 2 illustrates templates obtained for detecting the Reaction time to the Go and Stop signal on the COM tracks in three different types of Stop trials. The comparable algorithm applied to the COP track is not illustrated.

The exacts instants of reaction to the Go and Stop signals of APA were identified as the minimum of the Euclidean distance between the previously described templates and the corresponding signals (Supplementary figure 2 B), calculated as follows:

$$D(t) = \sqrt{\sum_{k=1}^{K} (S(k+t) - T(k))^2} \; ; \qquad t \in \{1,2,\cdots,N\}$$

$$d_{min} = arg \min_{t} D(t)$$

.

Where S and T are the signal and template respectively, K is the length of template and N is the length of signals.

Stability index

Mechanical stability and balance are commonly measured in movement analysis using two parameters: extrapolated COM (XCoM) and BOS. Both indices are used in gait analysis to assess stability during the gait double support (Hof et al., 2005; Watson et al., 2021) or at gait termination (Conte et al., 2012) It is not, however, used in transient phases of limb progression, as in our study. Therefore, a specific SSRT stability index (SSRT_STi) for this experimental study was built and computed from two parameters, XCoM and BOS.

This index is calculated as the distance between the BOS centroid and the XCoM along the two directions A-P (x-axis) and M-L (y-axis):

$$SSRT\_STi(t)\begin{cases} SSRT\_STi_x(t) = \dfrac{\left|C_{BoS_x}(t) - XCoM_x(t)\right|}{\frac{1}{N}\sum_{i=1}^{N}\left|C_{BoS_x}(t) - p_{xi}\right|} \\ SSRT\_STi_y(t) = \dfrac{\left|C_{BoS_y}(t) - XCoM_y(t)\right|}{\frac{1}{N}\sum_{i=1}^{N}\left|C_{BoS_y}(t) - p_{yi}\right|} \end{cases}$$

where $XCoM_x(t)$, $XCoM_y(t)$, $C_{BoS_y}(t)$ and $C_{BoS_x}(t)$ are the instantaneous anteroposterior and mediolateral XCoM and centroids of BoS positions respectively, p_{xi} and p_{yi} are the vertices that defined the BoS's perimeter and N is the number of vertices that compose BoS's perimeter (N =11).

The XCoM is a concept derived from a linearized inverted pendulum model, which can be considered as a point on the floor at a distance from the COM that is directly proportional to the COM velocity, and was calculated using the following formula:

$$XCoM(t)\begin{cases} XCOM_x(t) = CoM_x(t) + \dfrac{C\dot{o}M_x(t)}{\omega_0} \\ XCOM_y(t) = CoM_y(t) + \dfrac{C\dot{o}M_y(t)}{\omega_0} \end{cases}$$

where $XCOM_x(t)$, $XCOM_y(t)$ and $COM_x(t)$, $COM_y(t)$ are the instantaneous anteroposterior and mediolateral XCoM and CoM positions respectively, $C\dot{O}M_x(t)$ and $C\dot{O}M_z(t)$ are the instantaneous anteroposterior and mediolateral CoM velocities, and ω_0 is the natural frequency calculated by the following equation:

$$\omega_0 = \sqrt{\frac{g}{CoM_z(t)}}$$

where g is the acceleration of gravity and CoM_z is the effective height of the body's CoM above the floor.

Anthropometric measurements such as ankle, heel, and foot plant width (Supplementary figure 3A), were acquired for computing each participant's BoS.

The BoS, which in general refers to the area beneath the feet of a person and that includes every point with the supporting surface, in this research study was computed from foot markers and anthropometric measurements collected. In more detail, the BoS area's perimeter was defined instant by instant by the outermost feet markers (Supplementary figure 3B). Each marker was included or excluded from the set of those available for BoS calculation if its elevation (relative to its baseline) was smaller or greater than 5 mm, respectively.

Estimate of the Stop Signal Reaction Time according to the horse race model' assumptions

The mathematical approach used in this research project to estimate the SSRT was the integration method (Logan and Cowan, 1984). In depth, this method estimates the point at which the stop process finishes by 'integrating' the RT distribution and finding the point at which the integral equals probability of Stop Error trials. The finishing time of the stop process corresponds to the nth RT, with $n = number\ of\ RTs$ in the RT distribution of Go trials multiplied by $p(Stop\ Error)$.

STATISTICAL ANALYSIS

Repeated measures ANOVA was used to tests for significant of differences in APA Reaction time to the Go and Stop signal computed from COM, COP across the different trial types (Go, Stop Correct, Stop partial Error and Stop Error). Bonferroni's pot-hoc were performed for multiple comparisons.

A post-hoc statistical power analysis using G*Power (3.1.9.7) (Faul et al., 2009) was performed for ANOVA repeated measures, within factors, with α =0.05, based on partial eta squared (η_p^2) calculated by *F* (Lakens, 2013). The analysis indicated that the power (1-β err prob) for each ANOVA was > 0.95. The significance level was set to 0.05.

A correlation analysis (Pearson coefficient) was performed between each SSRT measured from COM, COP, and the SSRT estimated with the integration method.

References

Aron AR, Robbins TW, Poldrack RA. 2014. Inhibition and the right inferior frontal cortex: one decade on. *Trends Cogn Sci* **18**:177–185. doi:10.1016/j.tics.2013.12.003

Atsma J, Maij F, Gu C, Medendorp WP, Corneil BD. 2018. Active braking of whole-arm reaching movements provides single-trial neuromuscular measures of movement cancellation. *Journal of Neuroscience* **38**:4367–4382. doi:10.1523/JNEUROSCI.1745-17.2018

Bissett PG, Jones HM, Poldrack RA, Logan GD. 2021. Severe violations of independence in response inhibition tasks. *Sci Adv* **7**. doi:10.1126/sciadv.abf4355

Bonnetblanc F, Martin O, Teasdale N. 2004. Pointing to a target from an upright standing position: anticipatory postural adjustments are modulated by the size of the target in humans. *Neurosci Lett* **358**:181–184. doi:10.1016/j.neulet.2004.01.020

Brunamonti E, Chiricozzi FR, Clausi S, Olivito G, Giusti MA, Molinari M, Ferraina S, Leggio M. 2014. Cerebellar damage impairs executive control and monitoring of movement generation. *PLoS One* **9**. doi:10.1371/journal.pone.0085997

Brunamonti E, Ferraina S, Paré M. 2012. Controlled movement processing: Evidence for a common inhibitory control of finger, wrist, and arm movements. *Neuroscience* **215**. doi:10.1016/j.neuroscience.2012.04.051

Brunamonti E, Paré M. 2023. Neuronal activity in posterior parietal cortex area LIP is not sufficient for saccadic eye movement production. *Front Integr Neurosci* **17**. doi:10.3389/fnint.2023.1251431

Conte C, Serrao M, Casali C, Ranavolo A, Silvia M, Draicchio F, Di Fabio R, Monami S, Padua L, Iavicoli S, Sandrini G, Pierelli F. 2012. Planned Gait Termination in Cerebellar Ataxias. *The Cerebellum* **11**:896–904. doi:10.1007/s12311-011-0348-0

Cordo PJ, Nashner LM. 1982. Properties of postural adjustments associated with rapid arm movements. *J Neurophysiol* **47**:287–302. doi:10.1152/jn.1982.47.2.287

Davis RB, Õunpuu S, Tyburski D, Gage JR. 1991. A gait analysis data collection and reduction technique. *Hum Mov Sci* **10**:575–587. doi:10.1016/0167-9457(91)90046-Z

Day BL, Bancroft MJ. 2018. Voluntary steps and gait initiation, 1st ed, Balance, Gait, and Falls. Elsevier B.V. doi:10.1016/B978-0-444-63916-5.00006-9

de Jong R, Coles MGH, Logan GD, Gratton G. 1990. In search of the point of no return: The control of response processes. *J Exp Psychol Hum Percept Perform* **16**:164–182. doi:10.1037/0096-1523.16.1.164

de Leva P. 1996. Adjustments to Zatsiorsky-Seluyanov's segment inertia parameters. *J Biomech* **29**:1223–1230. doi:10.1016/0021-9290(95)00178-6

Emeric EE, Brown JW, Boucher L, Carpenter RHS, Hanes DP, Harris R, Logan GD, Mashru RN, Paré M, Pouget P, Stuphorn V, Taylor TL, Schall JD. 2007. Influence of history on saccade countermanding performance in humans and macaque monkeys. *Vision Res* **47**:35–49. doi:10.1016/j.visres.2006.08.032

Faul F, Erdfelder E, Buchner A, Lang A-G. 2009. Statistical power analyses using G*Power 3.1: Tests for correlation and regression analyses. *Behav Res Methods* **41**:1149–1160. doi:10.3758/BRM.41.4.1149

Gallagher R, Perez S, DeLuca D, Kurtzer I. 2021. Anticipatory weight shift between arms when reaching from a crouched posture. *J Neurophysiol* **126**:1361–1374. doi:10.1152/jn.00644.2020

Gan Huang, Dingguo Zhang, Xidian Zheng, Xiangyang Zhu. 2010. An EMG-based handwriting recognition through dynamic time warping2010 Annual International Conference of the IEEE Engineering in Medicine and Biology. IEEE. pp. 4902–4905. doi:10.1109/IEMBS.2010.5627246

Goonetilleke SC, Wong JP, Corneil BD. 2012. Validation of a within-trial measure of the oculomotor stop process. *J Neurophysiol* **108**:760–770. doi:10.1152/jn.00174.2012

Gutierrez-Farewik EM, Bartonek Å, Saraste H. 2006. Comparison and evaluation of two common methods to measure center of mass displacement in three dimensions during gait. *Hum Mov Sci* **25**:238–256. doi:10.1016/j.humov.2005.11.001

Hannah R, Aron AR. 2021. Towards real-world generalizability of a circuit for action-stopping. *Nat Rev Neurosci* **22**:538–552. doi:10.1038/s41583-021-00485-1

Hof AL, Gazendam MGJ, Sinke WE. 2005. The condition for dynamic stability. *J Biomech* **38**:1–8. doi:10.1016/j.jbiomech.2004.03.025

Houk JC, Bastianen C, Fansler D, Fishbach A, Fraser D, Reber PJ, Roy SA, Simo LS. 2007. Action selection and refinement in subcortical loops through basal ganglia and cerebellum. *Philosophical Transactions of the Royal Society B: Biological Sciences* **362**:1573–1583. doi:10.1098/rstb.2007.2063

Jana S, Hannah R, Muralidharan V, Aron AR. 2020. Temporal cascade of frontal, motor and muscle processes underlying human action-stopping. *Elife* **9**. doi:10.7554/eLife.50371

Jana S, Murthy A. 2018. Task context determines whether common or separate inhibitory signals underlie the control of eye-hand movements. *J Neurophysiol* **120**:1695–1711. doi:10.1152/jn.00085.2018

Jankowska E, Edgley S. 1993. Chapter 15 Interactions between pathways controlling posture and gait at the level of spinal interneurones in the cat. pp. 161–171. doi:10.1016/S0079-6123(08)62274-8

Kalidindi HT, Crevecoeur F. 2023. Human reaching control in dynamic environments. *Curr Opin Neurobiol* **83**:102810. doi:10.1016/j.conb.2023.102810

Lakens D. 2013. Calculating and reporting effect sizes to facilitate cumulative science: a practical primer for t-tests and ANOVAs. *Front Psychol* **4**. doi:10.3389/fpsyg.2013.00863

Leonard JA, Brown RH, Stapley PJ. 2009. Reaching to Multiple Targets When Standing: The Spatial Organization of Feedforward Postural Adjustments. *J Neurophysiol* **101**:2120–2133. doi:10.1152/jn.91135.2008

Lepers R, Breni◆re Y. 1995. The role of anticipatory postural adjustments and gravity in gait initiation. *Exp Brain Res* **107**. doi:10.1007/BF00228023

Logan GD, Cowan WB. 1984. On the ability to inhibit thought and action: A theory of an act of control. *Psychol Rev* **91**:295–327. doi:10.1037/0033-295X.91.3.295

Lord SR, Fitzpatrick RC. 2001. Choice stepping reaction time: A composite measure of falls risk in older people. *Journals of Gerontology - Series A Biological Sciences and Medical Sciences* **56**:627–632. doi:10.1093/gerona/56.10.M627

Lowrey CR, Nashed JY, Scott SH. 2017. Rapid and flexible whole body postural responses are evoked from perturbations to the upper limb during goal-directed reaching. *J Neurophysiol* **117**:1070–1083. doi:10.1152/jn.01004.2015

MacKinnon CD. 2018. Sensorimotor anatomy of gait, balance, and falls. pp. 3–26. doi:10.1016/B978-0-444-63916-5.00001-X

Massion J. 1994. Postural control system. *Curr Opin Neurobiol* **4**:877–887. doi:10.1016/0959-4388(94)90137-6

Middleton F. 2000. Basal ganglia and cerebellar loops: motor and cognitive circuits. *Brain Res Rev* **31**:236–250. doi:10.1016/S0165-0173(99)00040-5

Mille M-L, Creath RA, Prettyman MG, Johnson Hilliard M, Martinez KM, MacKinnon CD, Rogers MW. 2012. Posture and Locomotion Coupling: A Target for Rehabilitation Interventions in Persons with Parkinson's Disease. *Parkinsons Dis* **2012**:1–10. doi:10.1155/2012/754186

Mirabella G, Pani P, Ferraina S. 2011. Neural correlates of cognitive control of reaching movements in the dorsal premotor cortex of rhesus monkeys. *J Neurophysiol* **106**:1454–1466. doi:10.1152/jn.00995.2010

Mirabella G, Pani P, Paré M, Ferraina S. 2006. Inhibitory control of reaching movements in humans. *Exp Brain Res* **174**:240–255. doi:10.1007/s00221-006-0456-0

Mori S. 1987. Integration of posture and locomotion in acute decerebrate cats and in awake, freely moving cats. *Prog Neurobiol* **28**:161–195. doi:10.1016/0301-0082(87)90010-4

Muscillo R, Schmid M, Conforto S, D'Alessio T. 2011. Early recognition of upper limb motor tasks through accelerometers: real-time implementation of a DTW-based algorithm. *Comput Biol Med* **41**:164–172. doi:10.1016/j.compbiomed.2011.01.007

Olivito G, Brunamonti E, Clausi S, Pani P, Chiricozzi FR, Giamundo M, Molinari M, Leggio M, Ferraina S. 2017. Atrophic degeneration of cerebellum impairs both the reactive and the proactive control of movement in the stop signal paradigm. *Exp Brain Res* **235**. doi:10.1007/s00221-017-5027-z

Oudre L, Barrois-Müller R, Moreau T, Truong C, Vienne-Jumeau A, Ricard D, Vayatis N, Vidal P-P. 2018. Template-Based Step Detection with Inertial Measurement Units. *Sensors* **18**:4033. doi:10.3390/s18114033

Pani P, Giamundo M, Giarrocco F, Mione V, Fontana R, Brunamonti E, Mattia M, Ferraina S. 2022. Neuronal population dynamics during motor plan cancellation in nonhuman primates. *Proceedings of the National Academy of Sciences* **119**. doi:10.1073/pnas.2122395119

Paré M, Hanes DP. 2003. Controlled movement processing: superior colliculus activity associated with countermanded saccades. *J Neurosci* **23**:6480–9.

Pijnappels M, Delbaere K, Sturnieks DL, Lord SR. 2010. The association between choice stepping reaction time and falls in older adults-a path analysis model. *Age Ageing* **39**:99–104. doi:10.1093/ageing/afp200

Rab G, Petuskey K, Bagley A. 2002. A method for determination of upper extremity kinematics. *Gait Posture* **15**:113–119. doi:10.1016/S0966-6362(01)00155-2

RANAVOLO A, VARRECCHIA T, RINALDI M, SILVETTI A, SERRAO M, CONFORTO S, DRAICCHIO F. 2017. Mechanical lifting energy consumption in work activities designed by means of the "revised NIOSH lifting equation." *Ind Health* **55**:444–454. doi:10.2486/indhealth.2017-0075

Raud L, Thunberg C, Huster RJ. 2022. Partial response electromyography as a marker of action stopping. *Elife* **11**. doi:10.7554/eLife.70332

Rogers MW, Kukulka CG, Brunt D, Cain TD, Hanke TA. 2001. The influence of stimulus cue on the initiation of stepping in young and older adults. *Arch Phys Med Rehabil* **82**:619–624. doi:10.1053/apmr.2001.20833

Rydalch G, Bell HB, Ruddy KL, Bolton DAE. 2019. Stop-signal reaction time correlates with a compensatory balance response. *Gait Posture* **71**:273–278. doi:10.1016/j.gaitpost.2019.05.015

Scangos KW, Stuphorn V. 2010. Medial Frontal Cortex Motivates But Does Not Control Movement Initiation in the Countermanding Task. *The Journal of Neuroscience* **30**:1968–1982. doi:10.1523/JNEUROSCI.4509-09.2010

Schall JD, Palmeri TJ, Logan GD. 2017. Models of inhibitory control. *Philosophical Transactions of the Royal Society B: Biological Sciences* **372**:20160193. doi:10.1098/rstb.2016.0193

Skippen P, Matzke D, Heathcote A, Fulham WR, Michie P, Karayanidis F. 2019. Reliability of triggering inhibitory process is a better predictor of impulsivity than SSRT. *Acta Psychol (Amst)* **192**:104–117. doi:10.1016/j.actpsy.2018.10.016

St George Rebecca J., Fitzpatrick RC, Rogers MW, Lord SR. 2007. Choice stepping response and transfer times: Effects of age, fall risk, and secondary tasks. *Journals of Gerontology - Series A Biological Sciences and Medical Sciences* **62**:537–542. doi:10.1093/gerona/62.5.537

St George R. J., Fitzpatrick RC, Rogers MW, Lord SR. 2007. Choice Stepping Response and Transfer Times: Effects of Age, Fall Risk, and Secondary Tasks. *J Gerontol A Biol Sci Med Sci* **62**:537–542. doi:10.1093/gerona/62.5.537

Suzuki Y. 1995. Self-organizing QRS-wave recognition in ECG using neural networks. *IEEE Trans Neural Netw* **6**:1469–1477. doi:10.1109/72.471381

Takakusaki K. 2017. Functional Neuroanatomy for Posture and Gait Control. *J Mov Disord* **10**:1–17. doi:10.14802/jmd.16062

Takakusaki K. 2013. Neurophysiology of gait: From the spinal cord to the frontal lobe. *Movement Disorders* **28**:1483–1491. doi:10.1002/mds.25669

Uemura K, Oya T, Uchiyama Y. 2013. Gait & Posture Effects of visual interference on initial motor program errors and execution times in the choice step reaction. *Gait Posture* **38**:68–72. doi:10.1016/j.gaitpost.2012.10.016

Verbruggen F, Aron AR, Band GP, Beste C, Bissett PG, Brockett AT, Brown JW, Chamberlain SR, Chambers CD, Colonius H, Colzato LS, Corneil BD, Coxon JP, Dupuis A, Eagle DM, Garavan H, Greenhouse I, Heathcote A, Huster RJ, Jahfari S, Kenemans JL, Leunissen I, Li C-SR, Logan GD, Matzke D, Morein-Zamir S, Murthy A, Paré M, Poldrack RA, Ridderinkhof KR, Robbins TW, Roesch M, Rubia K, Schachar RJ, Schall JD, Stock A-K, Swann NC, Thakkar KN, van der Molen MW, Vermeylen L, Vink M, Wessel JR, Whelan R, Zandbelt BB, Boehler CN. 2019. A consensus guide to capturing the ability to inhibit actions and impulsive behaviors in the stop-signal task. *Elife* **8**. doi:10.7554/eLife.46323

Watson F, Fino PC, Thornton M, Heracleous C, Loureiro R, Leong JJH. 2021. Use of the margin of stability to quantify stability in pathologic gait – a qualitative systematic review. *BMC Musculoskelet Disord* **22**:597. doi:10.1186/s12891-021-04466-4

Wu G, Cavanagh PR. 1995. ISB recommendations for standardization in the reporting of kinematic data. *J Biomech* **28**:1257–1261. doi:10.1016/0021-9290(95)00017-C

Yiou E, Caderby T, Delafontaine A, Fourcade P, Honeine J-L. 2017. Balance control during gait initiation: State-of-the-art and research perspectives. *World J Orthop* **8**:815–828. doi:10.5312/wjo.v8.i11.815

Yitayeh A, Teshome A. 2016. The effectiveness of physiotherapy treatment on balance dysfunction and postural instability in persons with Parkinson's disease: a systematic review and meta-analysis. *BMC Sports Sci Med Rehabil* **8**:17. doi:10.1186/s13102-016-0042-0

Zatsiorsky VM, Aktov AV. 1990. Biomechanics of highly precise movements: The aiming process in air rifle shooting. *J Biomech* **23**:35–41. doi:10.1016/0021-9290(90)90039-6

Supplementary Material

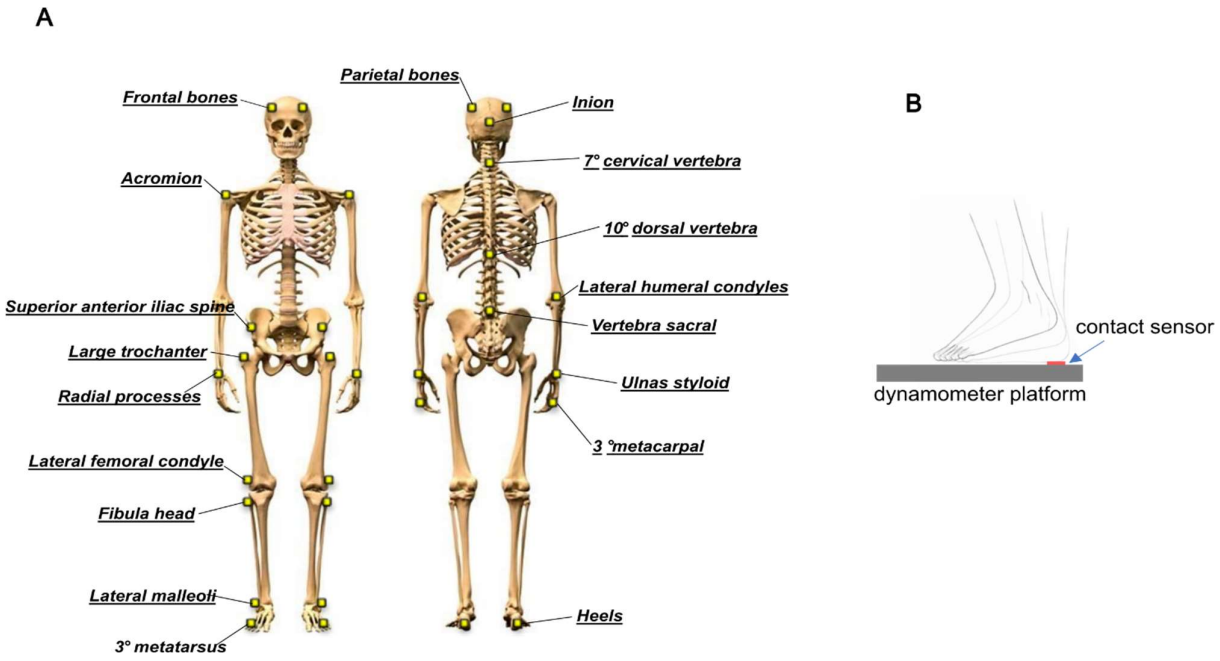

Supplementary figure 1 Schematic of devices for detection of behavioral, kinetic, and kinematic variables. A, displacement of kinematic sensors on the body target points. B, Relationship between foot, contact sensor and force detection platform.

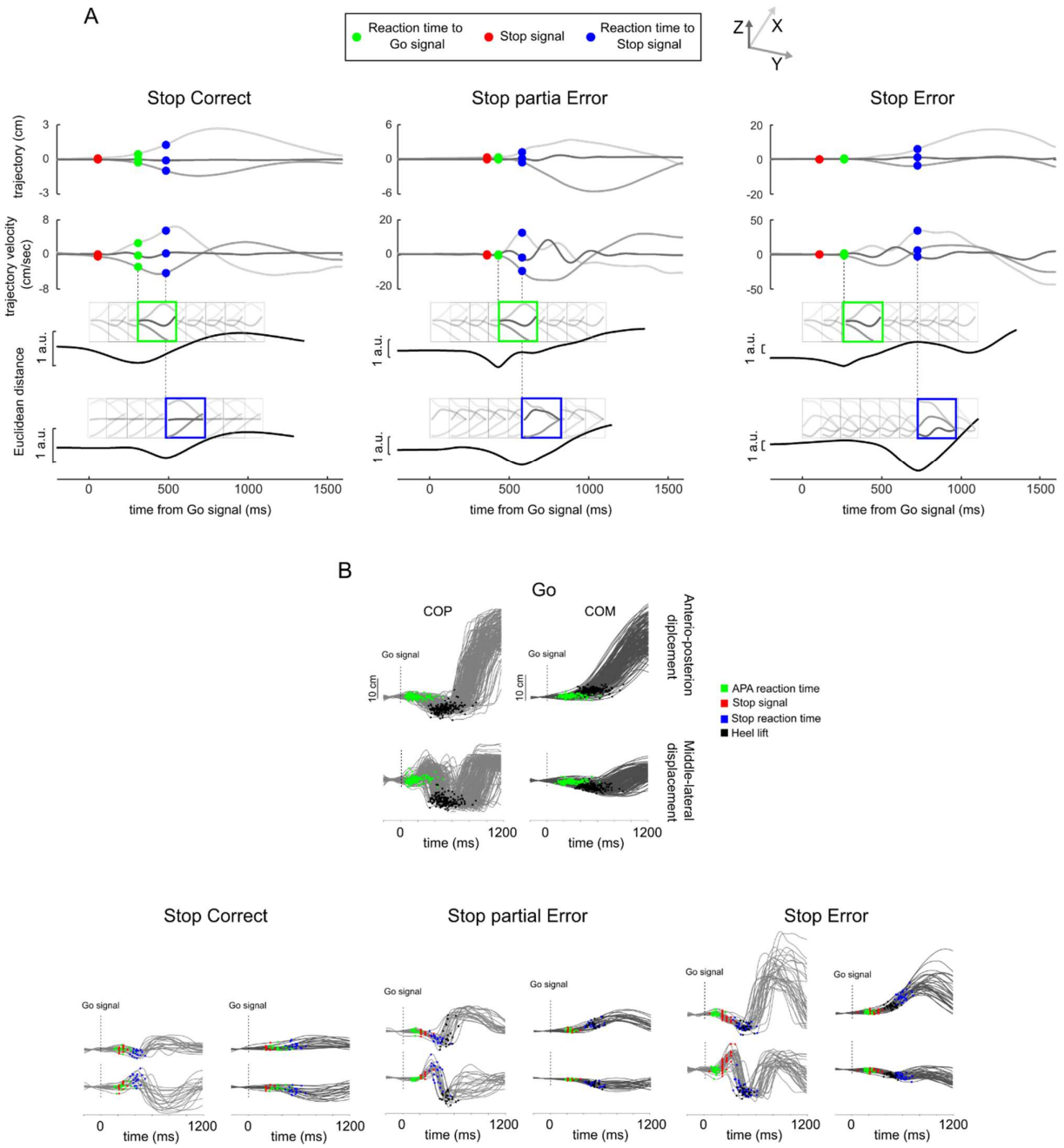

Supplementary figure 2

Single trial-based computation of reaction time to Go and Stop signal in Stop trials on COM A Upper row over time displacement of the X, Y and Z component of COM. Bottom rows velocity of X, Y and Z components of COM for each type of stop trial. The figure highlights the Euclidean distance between template of the pattern of change in velocity when participants reacted to the Go (Green rectangles) and Stop (Blue rectangles) signal. The reaction time to the Go and Stop signal is taken as the minimum Euclidean distance between the template and the velocity tracks (green and blue dots). B) time course of the Antero-posterior (upper plots) and (Mediolateral) shifting of a single trial of the four possible outcomes in the task the COP (left column) and COM (right column) of a participant performing the task. Each

line corresponds to a single trial of the four possible task's outcomes. Green squares and circles mark for each trial the time of APA onset obtained by the COP and COM respectively by applying the method illustrated in A.

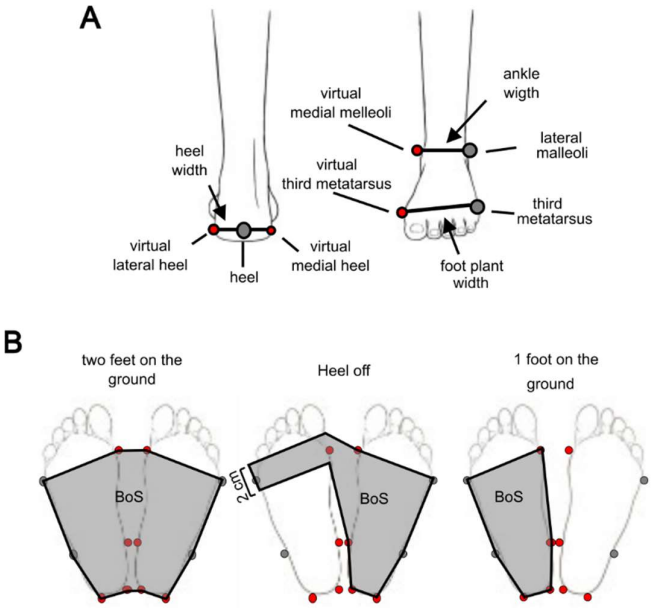

Supplementary figure 3

Computation of base of support. A, Anthropometric measures used for the computation of subjects' base of support. B, Three possible scenarios during gait initiation and their supporting bases are depicted schematically: 1) BoS when participants have both feet on the ground (leftmost panel); 2) BoS when participants are in the heel-off phase (middle panel); 3) BoS when participants have only one foot on the ground (rightmost panel).